1. Bilal ATTALLAH[1*], 2. Youcef BRIK[1] , 3. Abdelwahhab BOUDJELAL[1], 4. Hani BENGUESMIA[2]

Department of Electronics, LASS Laboratory, Faculty of Technology, University of M'sila, M'sila 28000, Algeria. (1)
Department of Electronics, LGE Laboratory, Faculty of Technology, University of M'sila, M'sila 28000, Algeria. (1)
LGE Laboratory, Faculty of Technology, University of M'sila, M'sila 28000, Algeria. (2)
ORCID: 1. 0000-0003-3661-957X; 2. 0000-0003-1565-0594; 3. 0000-0002-5704-1909; 4. 0000-0003-0437-1194

doi:10.15199/48.2024.09.10

Gabor, LBP, and BSIF features: Which is more appropriate for finger-knuckles-print recognition?

Abstract. *An accurate personal identification system helps control access to secure information and data. Biometric technology mainly focuses on the physiological or behavioural characteristics of the human body. This paper investigates the Finger Knuckle Print (FKP) biometric device based on the feature extraction technique. This FKP authentication method includes all the essential processes, such as preprocessing, feature extraction and classification. The features of the FKP application are investigated. Finally, this paper proposes the selection of the best feature extraction based on FKP recognition efficiency. The primary purpose of this paper is to use the Local Binary Patterns (LBP), Binarized Statistical Image Features (BSIF), and Gabor filters and define which helps to increase the False Acceptability Rate (FAR) and Genuine Acceptability Rate (GAR). This latest FKP selection shows better results as this concept shows promising results in recognizing a person's fingerknuckle print.*

Streszczenie. *Dokładny system identyfikacji osobistej pomaga kontrolować dostęp do bezpiecznych informacji i danych. Technologia biometryczna koncentruje się głównie na cechach fizjologicznych lub behawioralnych ludzkiego ciała. W artykule zbadano urządzenie biometryczne typu Finger Knuckle Print (FKP) oparte na technice ekstrakcji cech. Ta metoda uwierzytelniania FKP obejmuje wszystkie niezbędne procesy, takie jak przetwarzanie wstępne, ekstrakcja cech i klasyfikacja. Badane są funkcje aplikacji FKP. Na koniec w artykule zaproponowano wybór najlepszej ekstrakcji cech w oparciu o efektywność rozpoznawania FKP. Głównym celem tego artykułu jest wykorzystanie lokalnych wzorców binarnych (LBP), binarnych cech obrazu statystycznego (BSIF) i filtrów Gabora oraz zdefiniowanie, które pomagają zwiększyć współczynnik fałszywej akceptowalności (FAR) i współczynnik prawdziwej akceptowalności (GAR). Najnowsza selekcja FKP zapewnia lepsze wyniki, ponieważ koncepcja ta zapewnia obiecujące wyniki w rozpoznawaniu odcisków palców danej osoby. (**Funkcje Gabor, LBP i BSIF: Która z nich jest bardziej odpowiednia do rozpoznawania odcisków palców i kostek?)***

Keywords: Biometric Technology, Finger Knuckle Print (FKP), Local Binary Patterns (LBP), Genuine Acceptability Rate (GAR).
Słowa kluczowe: Technologia biometryczna, odcisk palca (FKP), lokalne wzorce binarne (LBP), rzeczywisty współczynnik akceptowalności (GAR).

Introduction

Applications for personal authentication can be found in many essential areas, including forensics, industry, and government services. Researchers are motivated to develop newer biometric modalities due to the exponential demand for Biometrics with lower spoofing susceptibility and superior usability. Determining which physiological or behavioural trait to use as a biometric depends on the security application, how easy and convenient it is to collect the data, how accurate it can be, etc. Several Biometrics, including fingerprints [1, 2], ear [3], face [5, 6], hand vein infrared programs [7, 8, 9], hand geometry [10], and many more, have already received a significant amount of research, which has given them a prominent position in society. The author's attention has been drawn to the promising biometric properties of the finger knuckle [11] and the fingernail plate [12]. The current study initially focused on the FKP score level fusion-based personal authentication (Finger-Knuckle-Print). This study aims to propose and provide an additional secure biometric-based personal authentication method. These are the novelties of our work.

In 2007, Hung-Ae Park introduced the concept of iris recognition, specifically emphasizing score-level fusion[13]. This approach involves analyzing the variation in frequency values of Log Gabor filters and utilizing the Hamming distance and Support Vector Machine (SVM) classification to explain the enrolled template. Enhancements are required for all other iris recognition algorithms to optimize the selection of the most efficient filters. Consequently, both the size of the retrieved feature and the time required for processing are significantly enhanced. During this occurrence, Alexandre Kowalczyk [14] proposed that the SVM should be specifically tailored towards mathematical applications in text categorization, picture recognition, and bioinformatics. In addition, he elaborated on the concept of the kernel's trick and the intricacies of the optimization problem.

Norman Poh [15] proposed a method that utilizes fusion scores to enhance the overall accuracy of the gadget. The system can enhance performance and accuracy by utilizing several protocols and integrating with the multimodal or intermodal domain. This is achieved by employing the same features and employing different classifiers. In order to overcome the performance limitations of individual matches, KarthikNandakumar [16] discusses the multi-biometric systems that successfully combine the data from different scores. This paper suggests the ideal combination of match scores according to the likelihood ratio and an evolving structure. Anil K. Jain [1] proposed the usage of a multimodal biometric system due to its superior recognition performance compared to a unimodal system. Due to its accessibility and score combination, this standard method generates a wide range of matches. He integrated the score matching into the information fusion he created. The fusion technique was invented by Mingxing He [17] using a combination of unimodal devices. The results of score-level fusions are computed based on support vector machines and the sum rule. Higher accuracy results from novel standardization techniques like (High- score reduction effect normalization). It is necessary to meticulously choose and compare the parameters, while computing the corresponding score densities. Using FKP image extraction, Hang [18] illustrated local and global knowledge features. The orientation feature, which consists of data from Gabor filters, helps scale up the Gabor filters. They are linked to the time-frequency analysis system. These global and local features are matched using a weighted average based on time-frequency analysis. The convex directional map that combines the orientation and magnitude response of the Gabor filter code is described by KelaniNithish [19]. Therefore, the angular distance for matching is necessary in

order to quantify the sensitivity of a competing code map. Vapnik [20] discusses the groundbreaking SVM problem using a binary class that shows how the hyper-plane is set up to show both positive and negative instances.

Instead of the SVM type of classification, this paper proposed a groundbreaking FKP identification technique for selecting the best descriptor using Gabor, LBP, and BSIF. Previous research has mainly focused on feature extraction and SVM classification in the dataset for different fingerknuckle print types. All the efficiency metrics are calculated for different FKP forms. According to our literature review, this paper also uses the SVM classification method. Different fingerknuckle prints are used to measure the output parameters, such as accuracy and specificity. As a result, this research project is coordinated with Section 2, which presents a block diagram of the suggested related work, and Section 3, which describes the interaction between the feature extraction level and the experiment's performance. Sections 4 and 5 also include a discussion of. The criteria that follow.

FKP recognition system

Figure 1 shows the proposed method pipeline for FKP based on multi-feature extraction techniques. The plan consists of three steps.

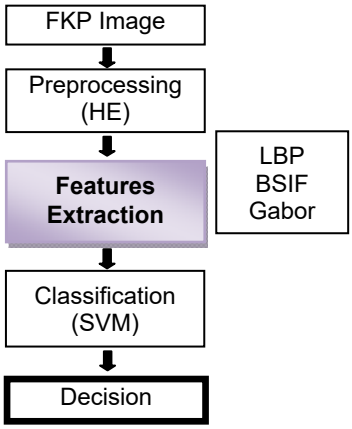

Fig.1. Proposed Method Pipeline.

FKP image preprocessing

Histogram equalization is applied to the input image to enhance the image qualities. Each pixel in the response pixel is replaced by the integral of the image's histogram.
In essence, histogram equalization refers to a form of difference modification using the image histogram in image processing.

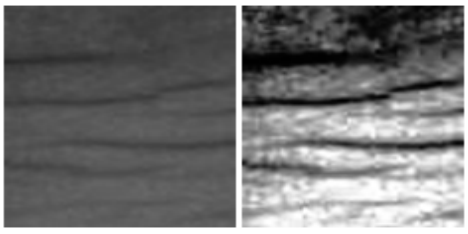

(a) (b)

Fig.2. FKP image preprocessing: (a) original FKP image, (b) enhanced FKP image.

The intensities on the histogram can be highly customized with this adjustment. As a result, the regions with the lowest local contrast are given a higher contrast.

Histogram equalization completes this by successfully spreading the most repeated intensity values. In addition, it has been observed that photographs with bright or dark backgrounds and foregrounds are advantageous, see Figure 1.
It can also perform differential adjustments to make image anomalies more transparent. The preprocessing function adapts the preprocessed image to the subsequent procedure [21].
Filter-based feature generation

1) Gabor features

The Gabor filter is utilized for the extraction of features at the designated point. The Gabor filter is capable of capturing both frequency and spatial uncertainty information simultaneously. When a bank of Gabor filters with various orientations and scales is applied to a ROI FKP image, it produces distinct Gabor features. Due to its invariance to illumination, rotation, size, and translation, the Gabor filter ensures a high level of consistency in the resulting Gabor features. The proposed methodology involves the extraction of magnitude data from FKP images through the utilization of a Gabor filter. The Gabor function utilized in this investigation [22] is defined as:

$$(1)\quad G(x,y)=\frac{f^2}{\pi\gamma\eta}\,e^{-\left(\frac{f^2x_1^2}{\gamma^2}+\frac{f^2y_1^2}{\eta^2}\right)}\,e^{j2\pi i f x_1}$$

Where: $x_1 = x\cos\theta + \sin\theta,\ y_1 = -x\sin\theta + y\cos\theta,$
f is the central frequency of the filter; *θ* is the orientation of the filter bank; *γ* is the sharpness along the x-axis, and *η* is the y-axis sharpness; Here, the centre of the filter is defined in polar coordinate with the parameter *(f, θ)*.

2) LBP features

This section describes the traditional feature extraction method that relies on block selection modes. Further details can be found in reference [23]. The binary code represents the feature value and multiscale texture analysis with varying values. The subsequent text provides a detailed explanation of the formula:

$$(2)\quad LBP_{P,R}=\sum_{p=0}^{p-1}s(g_p-g_c)2^p,\ s(x)=\begin{cases}1 & x\geq 0\\ 0 & x<0\end{cases}$$

g_c the grey value of the center pixel is represented by "G". Its neighbors are represented by "*P*", and the sampling radius is represented by "*R*".

The palmprint pictures are partitioned into blocks of *m* × *m* structure using a uniform LBP descriptor, which aligns with the traditional way of extracting texture features [24]. The feature vectors of each block are retrieved using the following formula:

$$(3)\quad h=\left\{h^1,h^2,.....,h^n\right\}$$

Where h is the total number of blocks, h n is the histogram for each block, and h is the final extracted feature vector. For example, the feature for this instance is extracted from a set of 16 blocks (n=16), each corresponding to a histogram with 16 16-bit histogram (dimensional feature vector). A 256- dimensional feature vector (16 ×16 = 256) results in the final uniform feature vector.

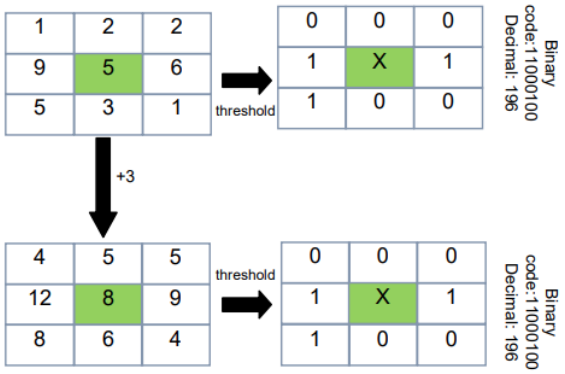

Fig.3.The Principal of LBP descriptor and Grey-Scale Invariant.

3) BSIF Features

Kannala et al. [25] proposed the introduction of BSIF. The method represents each pixel in an image using a binary code string. The code value of a pixel is considered as a local descriptor of the region of the image that is immediately surrounding it. Given an image I_P and a linear filter W_i of the same size, the filter response R_i is found by:

$$(4) \quad R_i = \sum_{m,n} I_p(m,n) W_i(m,n)$$

Where m and n refer to the PPI patch's size and the number of linear filters. ∀i = {1, 2, ..., n} whose responsecan be calculated and binarized to obtain the binary string as follows [16]:

$$(5) \quad b_i = \begin{cases} 1 & if \ R_i > 0 \\ 0 & otherwise \end{cases}$$

The texture features of the PPI can be clearly distinguished using the BSIF codes, which are displayed as a histogram of pixel binary codes. The practical evaluation of BSIF descriptors for palmprint verification depends on the filter size and bit string length.

In this study, four different bit lengths (6,7,9, and 11) were combined with eight different filter sizes (3 × 3, 5 ×5, 7×7,9×9,11×11,13×13,15×15, and 17×17) with four different bit lengths (6,7,9, and 11). (See Fig.2). The superior experimental accuracy obtained with this setup led to selecting the 17×17 filter with an 11-bit length.

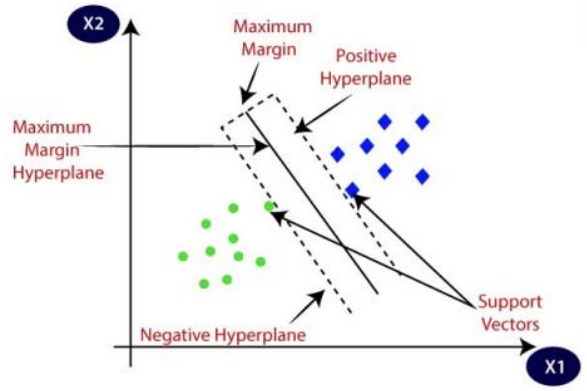

Fig. 4. Support Vector Machines (SVM) [20].

SVM multiclass classifier

The Support Vector Machine (SVM) is a classifier that is not based on probabilities. Its technical description involves the concept of a separating hyperplane. The approach utilizes the training data to build an optimal hyperplane that has a greater margin from the support vectors (supervised learning). A hyperplane is a straight line that separates a plane into two distinct classes in two-dimensional space (see to Figure 4). The SVM classifier's tuning parameters are epsilon, regularization, and kernel [20].

Experiment details

Dataset description

Our experiments were conducted using the IIT Delhi Finger-Knuckle-Image Version 1.0 (IITD) database [11] to evaluate the proposed system's verification accuracy and computational efficiency. With five images taken from the same finger for each subject, the IITD database

contains 790 grayscale finger-knuckle-print images (size = 80×100 pixels) from 158 subjects. Both images were used in the experiment. For preparation and research, the dataset is divided into two equal parts (50 per cent for each one).

Performance measurement

The confusion matrix is considered an effective tool for outlining the results of a model with classification problems [21]. In terms of classification, the prediction can be one of the following four specific circumstances:

The forecast is a True Positive if the classifier predicts that the object's verified worth is True and it is True in the dataset (TP). On the other hand, if the classifier predicts a False, the forecast is referredto as a False Negative (FN). In the same way, if the classifier predicts that an object's

The verified merit in the dataset is false, and the forecast is true negative (TN). On the other hand, if the forecast from the classifier is True, the prediction is false positive (FP) [26].

Determining the performance of the developed predictor becomes straightforward with the help of the confusion matrix, highlighted in Table 1.

Table 1. Confusion matrix for binary classification.

		Predicted values	
		0	1
Actual values	0	True Negative (TN)	False Positive (FP)
	1	False Negative (FN)	True Positive (TP)

The following metrics evaluate the suggested model [21], [26], [27].

- Accuracy (Acc): the proportion of accurate predictions a classifier made compared to the target's actual values during testing.

$$(6) \quad A_{CC} = \frac{(TP + TN)}{(TP + TN + FP + FN)} * 100\%$$

- Sensitivity (Sens): It provides data on the proportion of true positives correctly identified during the test.

$$(7) \quad Sens = \frac{TP}{(TP + FN)} * 100\%$$

- Specificity (Spec): It details true negatives detected and correctly categorized during the test.

$$(8) \quad Spec = \frac{TN}{(TP + TN)} * 100\%$$

- Precision (Pre): The proportion of cases the classifier has classified as positive out of all the predictive positives (the exactness of a classifier).

(9) $$\Pr e = \frac{TP}{(TP + FP)} * 100\%$$

- F1-score: It displays the precision and recall harmonic mean.

(10) $$F_1 - score = \frac{2 * TP}{(2 * TP + FN + FP)} * 100\%$$

Results and discussion

1) Gabor results

The first experiment defines the best parameters of Gabor features by trial and error. Since the training results of Gabor features at different parameters are the same with 100% accuracy, we consider only the testing results for choosing the optimal Gabor parameters).

Furthermore, we recall that the 2D Gabor filter applied on the FKP feature generation process is set to 39×39. Based on the results reported in Table 2, the optimal Gabor parameters a reset as follows: for the remaining experiments in this study, the number of scales is fixed at 7, and the number of orientations is fixed at 32. We recall that the final

Gabor feature-length results from multiplying the number of scales by the number of orientations. Table 3 displays the time it takes to compute Gabor features as a function of different parameters.

Table 2. Gabor feature testing results with different parameters

		N. orientations			
		8	**16**	**32**	**64**
N. scales	**3**	77.06	80.80	80.53	80.53
	5	92.00	93.06	92.80	92.80
	7	94.93	94.93	95.20	95.20
	9	91.73	92.80	92.80	92.80

Table 4 provides a comprehensive view of the performance of the Gabor feature for different sets of parameters, allowing for the selection of the optimal parameters for the desired performance metric.

2) LBP results

At this stage, we evaluate some tests to determine the optimal value of R (LBP mask radius) for LBP feature generation (see Table5). It is worth noting that we use an odd-sized mask to capture the local binary feature. For this purpose, we report the test results performed on the same FKP data set with different R parameter values. It is worth noting that the LBP feature vector length is 256, whatever the R-value. The values in Table 5 represent the performance of the Gabor feature in terms of the corresponding evaluation metric for the given set of parameters.

3) BSIF results

At this stage, we evaluate some tests to determine the optimal parameters of BSIF (see Tables7,8, and 9), such as the size of the texture filter and the number of codingbits. We note that the BSIF texture filter used is of odd size, varying from 5 to 17, while the number ofcodingbitsvariesfrom5to12.We report the test results obtained on the same FKP dataset with different values of the BSIF parameters. In addition, we recall that the final BSIF vector length is computedby2^N of the codingbits.

4) Comparative analysis

The statistics are reported in Table X to compare these three features in terms of different performance criteria.

Comparison with the state-of-the-art methods

We compare the results with approaches that used the same experimental protocol, performance measures, and FKP dataset to demonstrate where our three features stand in terms of performance. Table11 shows the outcomes of the three features compared to state-of-the-art methods.

Table 3. The time-consuming of Gabor features is a function of its parameters.

Parameters(Scales, orientations)	(**3**,**32**)	(**5**,**16**)	(**7**,**32**)	(**9**,**16**)	(**11**,**16**)	(**13**,**32**)
Feature generation time-consuming(s)	213.00	173.59	476.58	347.40	405.12	896.75
Training time con- summing(s)	2.93	2.77	3.89	3.71	3.67	7.40
Testing time con- summing(s)	0.40	0.32	0.94	1.01	0.69	1.39

Table 4.Gabor feature performance in testing

Performance (%)	(3,32)	(5,16)	(7,32)	(9,16)	(11,16)	(13,32)
Sensitivity	80.53	93.07	95.20	92.80	84.53	72.00
Specificity	99.87	99.95	99.97	99.95	99.90	99.81
Precision	80.53	93.07	95.20	92.80	84.53	72.00
NPV	99.87	99.95	99.97	99.95	99.90	99.81
FDR	19.47	06.93	04.80	07.20	15.47	28.00
FOR	00.13	00.04	00.03	00.04	00.10	00.19
TS	67.41	87.03	90.84	86.57	73.21	56.25
F1-score	80.53	93.07	95.20	92.80	84.53	72.00
MCC	80.40	93.02	95.17	92.75	84.43	71.81
FMI	80.53	93.07	95.20	92.80	84.53	72.00
Informedness	80.40	93.02	95.17	92.75	84.43	71.81
MK	80.40	93.02	95.17	92.75	84.43	71.81
Accuracy	99.74	99.91	99.94	99.90	99.79	99.63

Table 5.Testing results with different radius values of LBP mask.

R	3	5	7	9	11	13
Feature generation time con summing (s)	30.58	33.42	32.89	31.74	35.19	34.71
Training accuracy (%)	100	100	100	100	100	100
Training time(s)	5.52	4.33	4.75	5.21	4.27	4.21
Testing accuracy (%)	83.20	95.20	96.80	97.60	95.73	95.20
Testing time(s)	1.05	0.85	1.11	1.05	0.87	0.87

Table 6.Testing results with different combinations of BSIF parameters.

N. coding bits	5	6	7	8	9		10	11	12
Filter5x5	60.26	70.93	74.93	74.13	63.20		61.60	57.333	49.06
Filter7x7	74.40	84.00	87.20	88.80	90.13		88.26	86.40	84.53
Filter9x9	78.93	89.33	93.06	94.66	96.53		95.46	95.46	95.20
Filter1lxl1	82.13	90.66	94.40	96.26	97.06		97.60	98.40	98.66
Filter13xl3	84.80	90.13	95.46	96.53	98.66		98.66	99.20	99.46
Filter15x15	83.20	91.73	95.46	97.60	98.13		98.66	98.93	98.93
Filter17xl7	82.93	90.93	96.26	97.60	97.33		98.40	99.20	98.93

Table 7.The time-consuming BSIF features in the function of its parameters.

BSIF parameters	Filter 5x5 5 bits	Filter 5x5 12 bits	Filter 9x9 9 bits	Filter 11x1112 bits	Filter 13x1312 bits	Filter 17x1711 bits
Feature vector length	32	4096	512	4096	4096	2048
Feature generation time consuming(s)	3.82	8.07	6.37	11.37	13.23	15.00
Training accuracy (%)	100	100	100	100	100	100
Training time(s)	2.38	109.53	8.34	97.27	97.41	39.36
Testing accuracy (%)	60.26	49.06	96.53	98.66	99.46	99.20
Testing time(s)	0.24	31.82	1.81	28.08	28.77	7.42

Table 8. BSIF feature performances in testing.

Performance (%)	Filter5 ×55 bits	Filter5×512 bits	Filter9 ×99 bits	Filter11×1112 bits	Filter13×1312 bits	Filter17×17 11bits
Sensitivity	60.27	49.07	96.53	9867	99.47	99.20
Specificity	99.73	99.66	99.98	99.99	100	99.99
Precision	60.27	49.07	96.53	98.67	99.47	99.20
NPV	99.73	99.66	99.98	99.99	100	99.99
FDR	39.73	50.93	03.47	01.33	00.53	00.80
FOR	00.27	00.34	0.002	0.0008	0.0003	0.0005
TS	43.13	32.51	93.30	97.37	98.94	98.41
F1-score	60.27	49.07	96.53	98.67	99.47	99.20
MCC	60.00	48.72	96.51	98.66	99.46	99.19
FMI	60.27	49.07	96.53	98.67	99.47	99.20
Informedness	60.00	48.72	96.51	98.66	99.46	99.19
MK	60.00	48.72	96.51	98.66	99.46	99.19
Accuracy	99.47	99.32	99.95	99.98	99.99	99.99

Table 9. Comparison between Gabor, LBP, and BSIF features.

Performance (%)	Gabor(7,32)	LBP(R=9)	BSIF(13xl3,12bits)
Sensitivity	95.20	97.60	99.47
Specificity	99.97	99.98	100
Precision	95.20	97.60	99.47
NPV	99.97	99.98	100
FDR	04.80	02.40	00.53
FOR	00.03	00.01	0.0003
TS	90.84	95.31	98.94
F1-score	95.20	97.60	99.47
MCC	95.17	97.58	99.46
FMI	95.20	97.60	99.47
Informedness	95.17	97.58	99.46
MK	95.17	97.58	99.46
Accuracy	99.94	99.97	99.99

Table 10. Comparison with state-of-the-art in the case of FKP.

Methods	Recognition rate
Gabor+ PCA+LDA(face)[28]	75.25
Gabor+ Grav level intensity(fingerprint)[29]	88.48
Gabor+ LBP(face)[30]	94.75
MSLBP+ PCA+ LDA(face)[31]	94.81
Gabor+ DBC(face)[32]	90.82
Gabor+ ITBCDBC(FKP)[33]	91.33
Gabor+ MDBC(FKP)[34]	93.73
Gabor+Fracta1(texture)[35]	97.29
Gabor+ SVM(FKP)proposed	97.60
LBP+SVM(FKP)proposed	95.20
BSIF+SVM(FKP)proposed	99.46

Conclusion

Unlike traditional methods, the biometric technology provides a multitude of advantages. This work specifically examines the recognition of FKP (Facial Keypoint) using SVM (Support Vector Machine), which is suggested to be used in combination with the fusion process of Gabor, BSIF, or LBP features. The different results obtained from single and double FKP feature extraction are merged at the feature extraction fusion stage. The achieved outcomes and precision are undeniably more dependable than previous methods and bolster the initial endeavor. For this purpose, it is recommended to use a biometric recognition system that utilizes FKP (Fingerprint Key Point) with fusion at a matching score level. This study can also enhance

monomodalbiometrics.This is in a dynamic architecture with multi-fusion regulations to varying security levels. In order to improve security, this project will be expanded to build a hybrid biometric system with FKP and other characteristics. Numerous non-rigid biometric factors, such as height, race, and hair type, can potentially enhance the system.

REFERENCES

[1] N. Nedjah, R. S. Wyant, L. M. Mourelle, and B. B. Gupta, “Efficient fingerprint matching on smart cards for high security and privacy in smart systems,” Information Sciences, vol. 479, pp. 622–639, 2019.

[2] A. Grocholewska-czuryło, M. Retinger, “Biometrics as an authentication method in a public key infrastructure,” in Przeglad Elektrotechniczny, 15(2017) N°1, 60-64.

[3] L. Chen and Z. Mu, “Partial data ear recognition from one sample per person,” IEEE Transactions on Human-Machine Systems, vol. 46, no. 6, pp. 799–809, 2016.

[4] A. Benzaoui, Y. Khaldi, R. Bouaouina, N. Amrouni, H. Alshazly, and A. Ouahabi, “A comprehensive survey on ear recognition: Databases, approaches, comparative analysis, and open challenges,” Neurocomputing, 2023.

[5] H. Sellahewa and S. A. Jassim, "Image-quality-based adaptive face recognition," IEEE Transactions on Instrumentation and Measurement, vol. 59, no. 4, pp. 805–813, 2010.

[6] D. M. Vo and S.-W. Lee, “Robust face recognition via hierarchical collaborative representation,”Information Sciences, vol. 432, pp. 332–346, 2018.

[7] D. Huang, Y. Tang, Y. Wang, L. Chen, and Y. Wang, "Hand-dorsal vein recognition by matching local features of multisource key points," IEEE Transactions on Cybernetics, vol. 45, no. 9, pp. 1823–1837, 2014.

[8] C.-L. Lin and K.-C. Fan, "Biometric verification using thermal images of palm-dorsal vein patterns," IEEE Transactions on Circuits and Systems for Video Technology, vol. 14, no. 2, pp. 199–213, 2004.

[9] H. Qin and M. A. El-Yacoubi, “Deep representation-based feature extraction and recovering for finger-vein verification," IEEE Transactions on Information Forensics and Security, vol. 12, no. 8, pp. 1816–1829, 2017.

[10] A. Kumar and Y. Zhou, “Human identification using finger images,” IEEE Transactions on image processing, vol. 21, no. 4, pp. 2228– 2244, 2011.

[11] A. Kumar and C. Ravikanth, “Personal authentication using finger knuckle surface,” IEEE Transactions on Information Forensics and Security, vol. 4, no. 1, pp. 98–110, 2009.

[12] A. Kumar, S. Garg, and M. Hanmandlu, “Biometric authentication using finger nail plates,” Expert systems with applications, vol. 41, no. 2, pp. 373–386, 2014.

[13] H.-A. Park and K. R. Park, “Iris recognition based on score level fusion by using SVM," Pattern Recognition Letters, vol. 28, no. 15, pp. 2019–2028, 2007.

[14] A. Kowalczyk, “Support vector machines succinctly,” SyncfusionInc, 2017.

[15] N. Poh and S. Bengio, “Database, protocols and tools for evaluating score-level fusion algorithms in biometric authentication,” Pattern Recognition, vol. 39, no. 2, pp. 223–233, 2006.

[16] K. Nandakumar, Y. Chen, S. C. Dass, and A. Jain, "Likelihood ratio- based biometric score fusion," IEEE Transactions on pattern analysis and machine intelligence, vol. 30, no. 2, pp. 342–347, 2007.

[17] M. He, S.-J. Horng, P. Fan, R.-S. Run, R.-J. Chen, J.-L. Lai,M. K. Khan, and K. O. Sentosa, “Performance evaluation of score level fusion in multimodal biometric systems,” Pattern Recognition, vol. 43, no. 5, pp. 1789–1800, 2010.

[18] . Zhang, L. Zhang, D. Zhang, and H. Zhu, "Ensemble of local and global information for finger–knuckle-print recognition," Pattern Recognition, vol. 44, no. 9, pp. 1990–1998, 2011.

[19] LK. Nitesh, N. Komal, and K. Neha, “Finger-knuckle-print: a biometric identifier,” Journal of Pattern Intelligence, vol. 2, no. 1, p. 26, 2012.

[20] V. N. Vapnik, “The nature of statistical learning,” Theory, 1995.

[21] T. R. Gadekallu, N. Khare, S. Bhattacharya, S. Singh, P. K. R. Maddikunta, and G. Srivastava, "Deep neural networks to predict diabetic retinopathy," Journal of Ambient Intelligence and Humanized Computing, pp. 1–14, 2020.

[22] A. Muthukumar and A. Kavipriya, “A biometric system based on Gabor feature extraction with SVM classifier for finger-knuckle-print," Pattern Recognition Letters, vol. 125, pp. 150–156, 2019.

[23] J. N. I. Shayeb, Z. Alqadi, and J. Nader, “Analysis of digital voice features extraction methods,” International Journal of Educational Research and Development, vol. 1, no. 4, pp. 49–55, 2019.

[24] B. Attallah, Y. Brik, Y. Chahir, M. Djerioui, and A. Boudjelal, “Fusing palmprint, finger-knuckle-print for bi-modal recognition system based on LBP and bsif,” in 2019 6th International Conference on Image and Signal Processing and their Applications (ISPA). IEEE, 2019, pp. 1–5.

[25] B. Attallah, Y. Chahir, and A. Serir, “Geometrical local image descriptors for palmprint recognition," in Image and Signal Processing: 8th International Conference, ICISP 2018, Cherbourg, France, July 2-4, 2018, Proceedings 8. Springer, 2018, pp. 419–426.

[26] L. Ali, A. Rahman, A. Khan, M. Zhou, A. Javeed, and J. A. Khan, “An automated diagnostic system for heart disease prediction based on x2 statistical model and optimally configured deep neural network,” Ieee Access, vol. 7, pp. 34 938–34 945, 2019.

[27] T. Beghriche, M. Djerioui, Y. Brik, B. Attallah, and S. B. Belhaouari, “An efficient prediction system for diabetes disease based on deep neural network,” Complexity, vol. 2021, pp. 1–14, 2021.

[28] P. Pirozmand, M. F. Amiri, F. Kashanchi, and N. Y. Layne, “Age estimation, a Gabor pca-lda approach,” The Journal of Mathematics and Computer Science, vol. 2, no. 2, pp. 233–240, 2011.

[29] S. Shan, W. Gao, Y. Chang, B. Cao, and P. Yang, “Review the strength of Gabor features for face recognition from the angle of its robustness to misalignment," in Proceedings of the 17th International Conference on Pattern Recognition, 2004. ICPR 2004., vol. 1. IEEE, 2004, pp. 338–341.

[30] X. Tan and B. Triggs, “Fusing Gabor and LBP feature sets for kernel-based face recognition," in Analysis and Modeling of Faces and Gestures: Third International Workshop, AMFG 2007 Rio de Janeiro, Brazil, October 20, 2007 Proceedings 3. Springer, 2007, pp. 235–249.

[31] M. Eismann, "Hyperspectral remote sensing." Society of Photo-Optical Instrumentation Engineers, 2012.

[32] H. Jagadeesh, K. S. Babu, and K. Raja, “Dbc based face recognition using dwt,” arXiv preprint arXiv:1205.1644, 2012.

[33] W. Nunsong and K. Woraratpanya, "Modified differential box-counting method using weighted triangle-box partition," in 2015 7th International Conference on Information Technology and Electrical Engineering (ICITEE). IEEE, 2015, pp. 221–226.

[34] W. Nunsong et al., “An improved finger-knuckle-print recognition using fractal dimension based on Gabor wavelet,” in 2016 13th International Joint Conference on Computer Science and Software Engineering (JCSSE). IEEE, 2016, pp. 1–5.

[35] A. G. Zuniga, J. B. Florindo, and O. M. Bruno, “Gabor wavelets combined with volumetric fractal dimension applied to texture analysis,” Pattern Recognition Letters, vol. 36, pp. 135–143, 2014